Soft-matter composites with electrically tunable elastic rigidity

2013 Smart Mater. Struct. 22 085005

(http://iopscience.iop.org/0964-1726/22/8/085005)

Smart Mater. Struct. **22** (2013) 085005 (8pp) doi:10.1088/0964-1726/22/8/085005

Soft-matter composites with electrically tunable elastic rigidity

Wanliang Shan, Tong Lu and Carmel Majidi

Soft Machines Lab, Department of Mechanical Engineering, Carnegie Mellon University, Pittsburgh, PA 15213, USA

E-mail: cmajidi@andrew.cmu.edu

Received 24 January 2013, in final form 20 June 2013
Published 9 July 2013
Online at stacks.iop.org/SMS/22/085005

Abstract
We use a phase-changing metal alloy to reversibly tune the elastic rigidity of an elastomer composite. The elastomer is embedded with a sheet of low-melting-point Field's metal and an electric Joule heater composed of a serpentine channel of liquid-phase gallium–indium–tin (Galinstan®) alloy. At room temperature, the embedded Field's metal is solid and the composite remains elastically rigid. Joule heating causes the Field's metal to melt and allows the surrounding elastomer to freely stretch and bend. Using a tensile testing machine, we measure that the effective elastic modulus of the composite reversibly changes by four orders of magnitude when powered on and off. This dramatic change in rigidity is accurately predicted with a model for an elastic composite. Reversible rigidity control is also accomplished by replacing the Field's metal with shape memory polymer. In addition to demonstrating electrically tunable rigidity with an elastomer, we also introduce a new technique to rapidly produce soft-matter electronics and multifunctional materials in several minutes with laser-patterned adhesive film and masked deposition of liquid-phase metal alloy.

(Some figures may appear in colour only in the online journal)

1. Introduction

Elastomers with electrically controlled stiffness have the potential to revolutionize robotics and assistive wearable technologies by allowing actuators to independently and reversibly change both their shape and elastic rigidity. Possible applications range from artificial muscles for humanoid and bio-inspired robots to spontaneously stiffening exoskeletons that prevent injury during collisions. Current methods for tunable stiffness require external pumps and valves for gel hydration [1, 2] and pneumatic particle jamming [3, 4], large electromagnets to activate magneto-rheological (MR) fluids [5, 6] and elastomers [7], and motors for variable stiffness springs [8]. While appropriate for relatively large machinery, these mechanisms cannot be easily scaled for clothing-embedded technologies, milli-robotics, and other applications that depend on miniaturization and autonomous operation. Instead, such applications require soft active materials that are intrinsically elastic, can be patterned into any shape, and are activated with the same electronics that power other on-board functionalities.

Reversible rigidity control has recently been demonstrated with laminar composites that contain either shape memory polymer (SMP) [9–11] or electroactive polymer (EAP) [12]. When heated above its glass transition temperature (T_g), the SMP softens and the flexural rigidity of the composite decreases by as much as 2–3 orders of magnitude [9–11]. In contrast to the current study, these variable stiffness composites do not incorporate a soft-matter Joule heating element to control temperature. Nonetheless, SMPs represent a promising alternative to low-melting-point metal alloys for applications that require less stiffness variation (2–3 orders of magnitude versus 3–4) and higher elastic rigidity when the composite is activated (1–10 MPa versus 0.1 MPa).

In this paper, we introduce a new class of rigidity tunable composites (RTCs) that combine a thermally responsive layer (e.g. SMP or a low-melting-point metal) with an elastically soft Joule heating element. Soft-matter Joule heating is accomplished with liquid-embedded elastomer electronics (LE3), an exciting new technology that combines soft microfluidics and soft lithography fabrication techniques

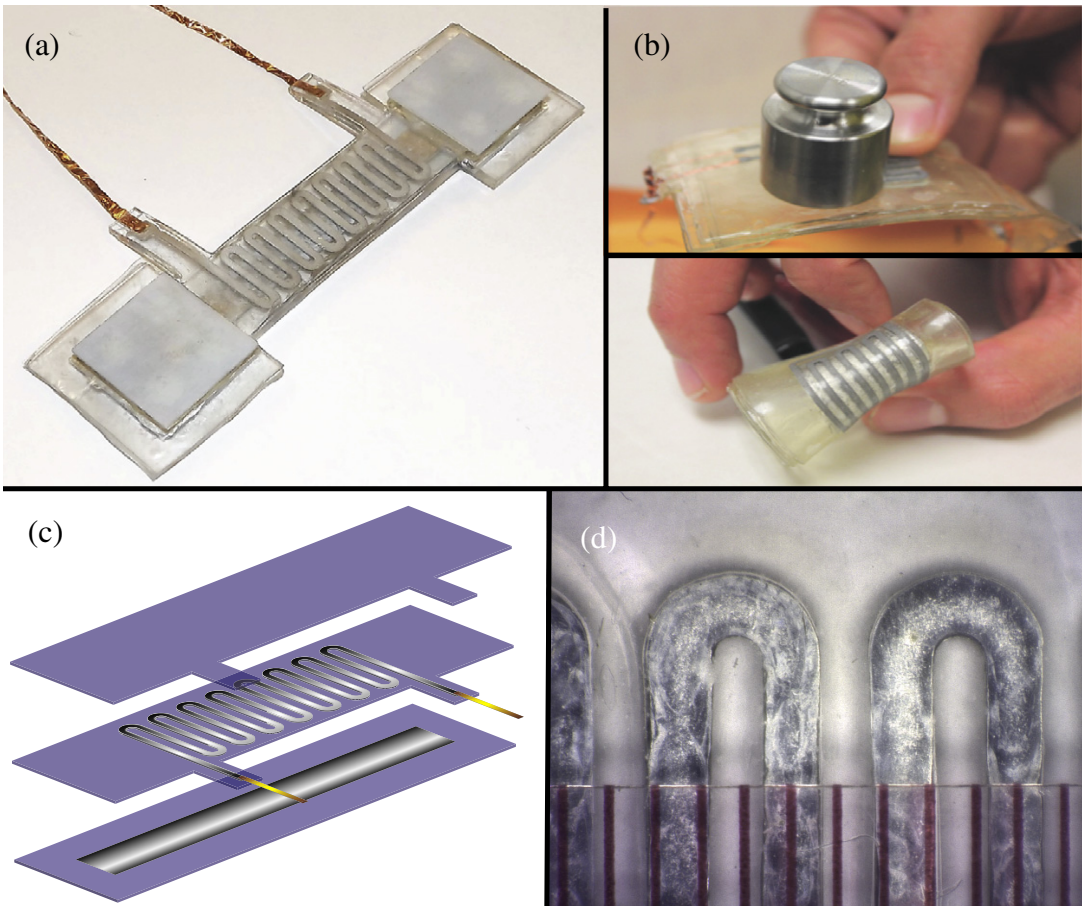

Figure 1. (a) Stiffness tunable composite embedded with Field's metal strip and liquid-phase Galinstan heater. (b) When electrically activated, the composite softens and easily deforms. (c) Illustration of the composite composed of a (top) elastomer sealing layer, (middle) liquid-phase Joule heating element, and (bottom) thermally activated layer of Field's metal or SMP. (d) Close-up of Galinstan heating element; ruler marks spaced 1 mm apart.

with liquid-phase metal alloy electronics [13, 14]. The soft-matter heater represents an extension of previous efforts to produce a flexible microcoil heater by embedding poly(dimethylsiloxane) (PDMS) elastomer with low-melting-point metal solder [15]. In order to allow the heater to be both flexible and stretchable, the solder is replaced with a gallium–indium alloy that is liquid at room temperature [13]. Also, instead of replica molding and injection filling, the LE3 heater is produced with masked deposition [16, 17]. This enables stiffness tunable composites to be produced rapidly and in combination with other soft-matter LE3 technologies through a single fabrication process.

To demonstrate RTC functionality with an LE3 heating element, we examine the dramatic rigidity change of a composite embedded with a sheet of low-melting-point Field's metal (figure 1(a)). This composite exhibits a dramatic and reversible change in its elastic rigidity when the embedded alloy melts through electric Joule heating (figure 1(b)). The effective Young's modulus E' of the composite is measured with a materials testing machine. At room temperature, the embedded Field's metal is solid and the modulus E' is governed by the rigidity of the solidified alloy. Activating the composite with 6 A of electrical current causes the alloy to melt and E' to decrease by four orders of magnitude. In this activated state, the composite becomes elastically soft and is free to stretch and bend. When power is removed (i.e. the heater is de-activated), the composite cools to room temperature and returns to its rigid state. In both states, the measured E' is in good agreement with theoretical predictions obtained from linear elasticity.

We also observe reversible rigidity control when replacing the Field's metal with a sheet of SMP. In this case, activating the Joule heater causes the embedded SMP film to heat up past its glass transition temperature T_g and allows the composite to soften elastically. Although the change in rigidity is not as dramatic as it is with Field's metal, SMP is a versatile and lightweight alternative that exhibits both reversible rigidity and shape change and can be easily incorporated into an RTC using the rapid prototyping method.

2. Design and fabrication

Referring to figure 1(c), the RTC is composed of an acrylic VHB elastomer sealing layer, a middle film containing two layers of VHB tape embedded with a liquid-phase Galinstan heating element, and a bottom thermally responsive layer. This bottom layer is composed of three layers of VHB tape

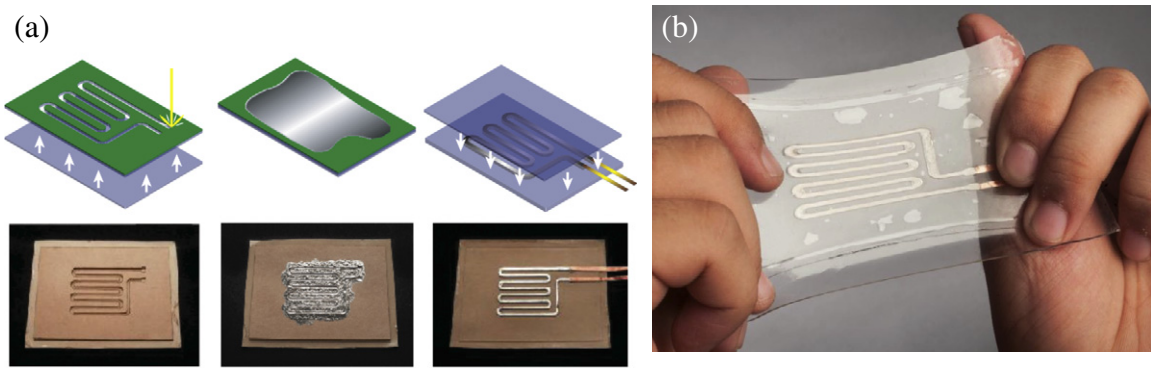

Figure 2. (a) Fabrication of a Galinstan heating element embedded in an acrylic VHB elastomer: (left) VHB film and liner are patterned with a laser engraver and bonded to a VHB substrate; (middle) sample is coated with Galinstan, which wets the exposed portions of the substrate; (right) the liner mask is removed and the patterned surface is sealed with a VHB film. (b) Liquid-phase Galinstan heater embedded in VHB elastomer.

embedded with a strip of Field's metal (RotoMetals, Inc.). The Galinstan heater (figure 1(d)) is activated with an external power supply that connects to the heater through a pair of copper shims. When powered, the Galinstan heater increases the temperature of the thermally responsive layer. The Field's metal melts when heated above its melting temperature T_m of 62 °C.

2.1. Fabrication method

We produce each layer of the composite using the masked deposition method presented in figure 2(a). First, we use a 30 W CO_2 laser engraver (VLS 3.50; Universal Laser Systems) to cut planar patterns in a sheet of VHB tape and liner film. After removing the excess tape, we bond the patterned sheet to a second layer of VHB tape. Next, we deposit liquid-phase Galinstan alloy, and remove the liner mask, leaving liquid alloy only in the exposed surface features. Lastly, we attach copper shim wires and seal the liquid by bonding a third layer of VHB tape. As demonstrated in figure 2(b), this method allows a liquid-phase Galinstan heater to be embedded in a thin sheet of VHB elastomer. Since the alloy is liquid at room temperature, the heater can be stretched to several times its natural length without losing functionality. Alternatively, instead of laser machining the middle layer of VHB film through the entire thickness, the film can instead be engraved with surface patterns. In this case, a bottom VHB substrate (as shown on the left of figure 2(a)) is not required and only a top sealing layer is necessary once the Galinstan is deposited and the liner mask is removed.

The Field's metal composite is $h_C = 4.5$ mm thick, $w_C = 15$ mm wide, and 50 mm long. It contains a rectangular strip of Field's metal that is $h_F = 1$ mm thick and $w_F = 7$ mm wide. The strip is produced by melting the Field's metal on a hotplate set to 100 °C and then depositing it on a laser-patterned sheet of VHB tape using the same fabrication steps (figure 2(a)) used to produce the liquid-phase heater. The heater contains a serpentine channel of Galinstan that is $w_G = 1.27$ mm wide, $h_G = 0.5$ mm deep, and 218.9 mm long. Each turn is approximately $L_t = 10$ mm long and spaced $s = 1.23$ mm apart. Referring to section 3, the Young's modulus of the VHB elastomer and Field's metal are $E_V = 128$ kPa and $E_F = 9.25$ GPa, respectively. Examples of the RTC with Field's metal are presented in figures 1(a) and (b).

Tensile tests were performed on the Field's metal composite specimens shown in figure 1(a). In addition to the Galinstan channel and Field's metal strip, these test specimens contain 3D-printed plastic attachments (Verowhite^{TM}; Objet Ltd) that are bolted to the ends of the Field's metal strip and allow the specimen to be fixed to a tensile testing machine.

2.2. Principles of operation

At room temperature, the RTC is rigid and can support external loading. In the electrically activated state, the composite softens and bends under light force (figure 1(b)). The elastic rigidity of the composite is quantified by its effective Young's modulus $E' = FL/uA$, where u is the displacement induced by stretching a prismatic specimen of length L and cross-sectional area A with a uniaxial tensile load F. As described in section 3, E' is measured experimentally with a tensile testing machine. However, the modulus E' can also be predicted with composite mechanics for both the non-active (off) and active (on) states,

$$E'_{off} = \left\{ \frac{\ell_G}{\alpha_F E_F + \alpha_{V1} E_V} + \frac{\ell_s}{\alpha_F E_F + \alpha_{V2} E_V} \right\}^{-1}, \quad (1)$$

$$E'_{on} = \left\{ \frac{\ell_G}{\alpha_{V1} E_V} + \frac{\ell_s}{\alpha_{V2} E_V} \right\}^{-1}, \quad (2)$$

where $\ell_G = w_G/(w_G+s)$, $\ell_s = s/(w_G+s)$, $\alpha_F = h_F w_F/h_C w_C$, $\alpha_{V1} = 1-\alpha_F-h_G L_t/h_C w_C$, and $\alpha_{V2} = 1-\alpha_F-h_G w_G/h_C w_C$. According to equations (1) and (2), activating the composite should cause E' to decrease by four orders of magnitude, from $E'_{off} = 0.959$ GPa to $E'_{on} = 109.2$ kPa.

The energy input needed to melt the Field's metal layer in the composite is estimated as

$$U = \rho_F \beta_F L_F + \sum_{i \in \{F,V,G\}} \rho_i c_i \beta_i \Delta T, \quad (3)$$

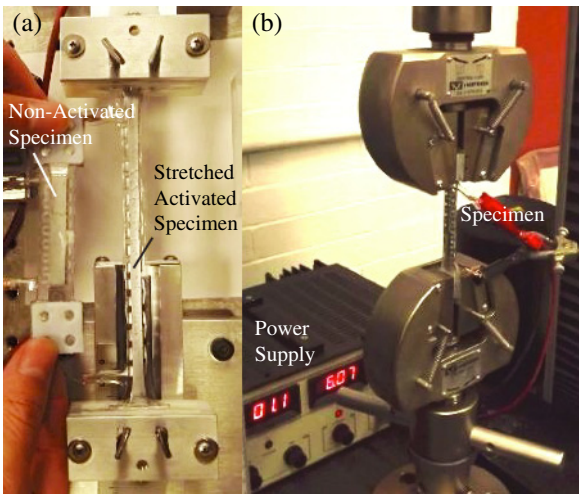

Figure 3. (a) A non-activated specimen and an electrically activated specimen that is stretched to twice its natural length. (b) An activated specimen loaded with a tensile tester.

where ρ_i is the density of the ith component of the composite, c_i the specific heat, β_i is the volume, L_F is the specific latent heat of the Field's metal, $\Delta T = T_m - T_0$, and $T_0 = 25\,^{\circ}\mathrm{C}$ is room temperature. The indices F, V, and G correspond to the Field's metal, VHB tape, and Galinstan channel, respectively. For a prescribed power input rate P, the time required to melt the Field's metal and activate the composite is approximately $t = U/P$. This estimate assumes a uniform temperature within the composite and ignores heat loss to the environment. VHB tape, Field's metal, and Galinstan have a density of 960, 9700, and 6440 kg m^{-3} and volume of 2837.5, 350, and 187.5 mm^3, respectively. The specific heat capacity and latent heat for these materials are unknown and so we instead use typical values for elastomers and low-melting-point alloys (Wood's metal): $c_V = 2010$ J kg^{-1} K^{-1}, $c_F = c_G = 172$ J kg^{-1} K^{-1}, and $L_F = 39\,980$ J kg^{-1}. Using these numbers, the activation energy is estimated to be $U = 370$ J, of which 135 J is the latent heat of Field's metal. So for example, with 3 W of power input, the composite will require approximately 2 min to completely soften.

3. Experimental method

The effective Young's modulus (E') of the composite was measured with a motorized tensile tester (Instron^{TM}, Norwood, MA), as shown in figure 3. The specimens were loaded with a 1 mm s^{-1} extension rate to a final extension of 7 mm (14% strain). Referring to figures 1(a) and 3(a), the composite specimens have a dog-bone shape with 4.5 mm × 15 mm rectangular cross sections and a gauge length of 50 mm. The samples also have wider rectangular shaped ends with through holes to allow for rigid clamping. We first performed measurements at room temperature, at which the Field's metal is solid and rigid. Next, we melted the Field's metal by supplying the composite with 6 A of electrical current and performed additional tensile measurements (figure 3(b)). The modulus E' is obtained by fitting linear regressions to the experimental stress–strain plots and calculating the slope.

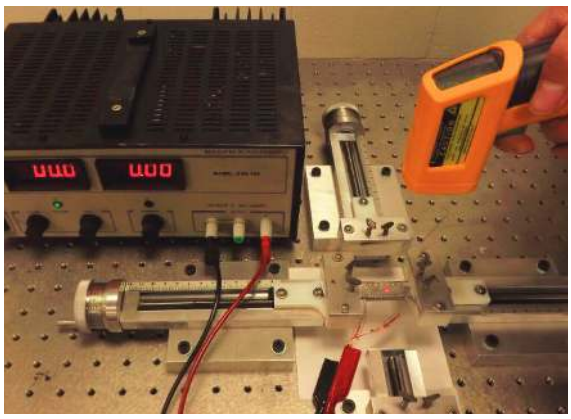

Figure 4. Experimental setup for measuring the composite surface temperature with an IR thermometer.

The theory in section 2.2 is based on independent measurements of the Young's modulus of VHB tape and room temperature Field's metal. For Field's metal, dog-bone specimens of different sizes were used to determine the Young's modulus. Five of these specimens had a size of 3 mm × 5 mm × 50 mm and the remaining four had dimensions of 3 mm × 5 mm × 91 mm. The Young's modulus of the Field's metal was measured to be 9.25 ± 0.60 GPa ($N = 9$). Similarly, the Young's modulus of VHB^{TM} tape was measured to be 128.4 ± 24.3 kPa ($N = 5$).

Temperature is measured with a Fluke 62 Mini IR thermometer (Fluke Corp. Everett, WA) as a function of time starting from when electrical power is supplied to the composite. The composite is initially at room temperature and is suspended on a mechanical stage to allow for free air convection (figure 4). These samples are either clamped at the ends to fixtures or suspended in air with the clamped ends removed and replaced by thin VHB strips (for the purpose of minimizing heat loss through contact). Next, the specimen is supplied with 6 A of electrical current using an external power supply. As shown in figure 4, an IR thermometer and a camera are used to record the temperature around the center of the bottom composite surface until the temperature reaches ∼90 °C. The temperature versus time profile is then extracted from the video. This profile is used to establish the time needed to complete the alloy phase change.

4. Results and discussion

Implementing the experimental steps described above, we measured the effective elastic modulus E' of the Field's metal composites. As shown in figure 3, the specimens are loaded with a tensile tester (Instron^{TM}; Norwood, MA) and activated with an external power supply. Stress–strain curves are presented in figure 5 for specimens in the non-active and active states. The effective Young's modulus E' is obtained by calculating the slope of the curve. At room temperature, the Field's metal is solid and $E'_{off} = 0.86 \pm 0.10$ GPa (sample number, $N = 9$) (figure 5(a)). When external power is supplied, the Field's metal melts and the effective Young's modulus of the composite reduces by four orders of magnitude

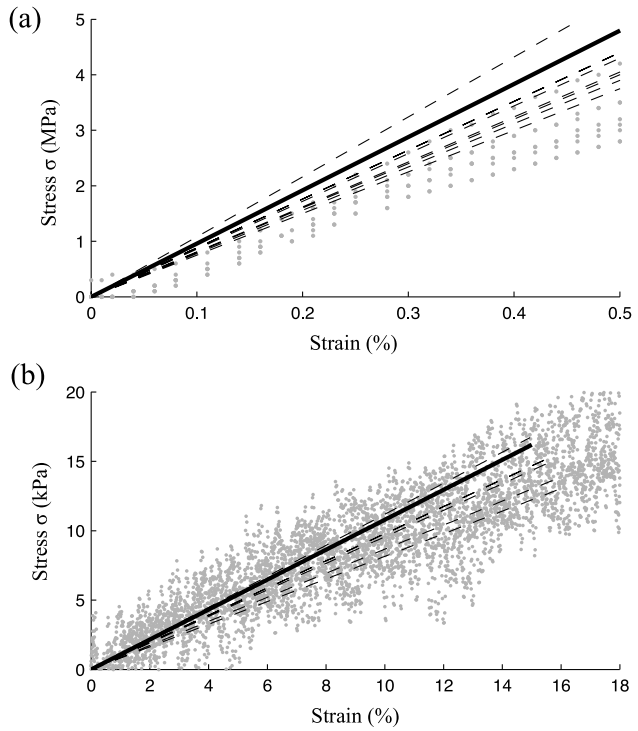

Figure 5. Stress–strain curves for (a) a non-activated specimen and (b) an activated specimen; (solid) theoretical predictions based on equations (1) and (2); (dashed) linear regression of experimental measurements (light gray markers). Agreement between the theory and experiment is accomplished without the aid of data fitting.

to $E'_{\text{on}} = 95.2 \pm 10.5$ kPa ($N = 6$) (figure 5(b)). A total of twelve samples were tested, three of which were tested in both the activated and non-activated states. As demonstrated in the figures, the experimental measurements are in reasonable agreement with the theoretical predictions obtained from equations (1) and (2).

The Galinstan channel in the Joule heating layer is 218.9 mm long, 1.27 mm wide, and 0.5 mm deep (figure 1(d)). Galinstan has a resistivity of $r = 2.9 \times 10^{-7}$ Ω m, so the total resistance is $R = 0.10$ Ω. The heater is activated with $i = 6$ A of current and thus consumes approximately $P = i^2R = 3.6$ W of power. Therefore, the composite is expected to require $t = U/P = 102.8$ s to be supplied with the $U = 370$ J of energy necessary to melt the Field's metal. This prediction is roughly consistent with the results presented in figure 6, which demonstrates that the heated alloy undergoes a phase change after approximately 130 s. This phase change corresponds to an inflection in the temperature profile—the rate at which the temperature increases slows down as T approaches T_{m} and then increases again when $T > T_{\text{m}}$.

There are several potential reasons why the theory underestimates the actual activation time. One factor is that the semicircular regions of the serpentine channel are wider than the rest of the channel and this will reduce the electrical resistance and power output of the Joule heater. Another factor is that when the Field's metal melts, the temperature of the heater will be much higher than that of the Field's metal layer. Therefore, the assumption that internal temperature is uniform will be violated and the actual energy required to complete

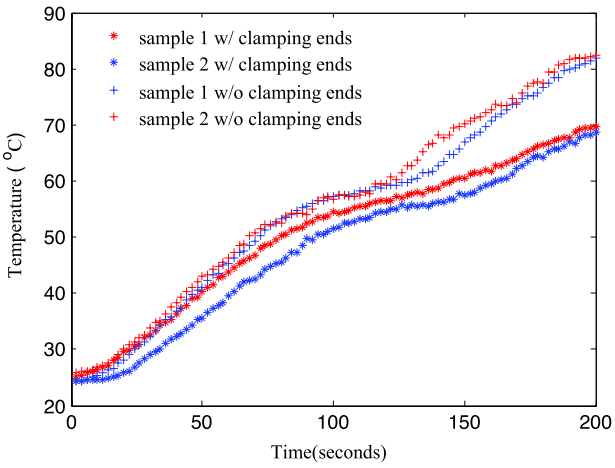

Figure 6. Time versus temperature for specimens activated with 6 A of current. Note that removing the clamping ends of the specimens reduced the time needed to induce phase change.

the melting will be greater than predicted. Nonetheless, as demonstrated in figure 6, the theory provides a reasonable estimate of the time it takes for the temperature T of the composite to reach the melting point $T_{\text{m}} = 62\,^{\circ}\text{C}$ of Field's metal.

The measurements performed with a tensile tester demonstrate that soft-matter composites composed of liquid-phase and phase-changing metal alloys are capable of dramatic changes in elastic rigidity. According to the stress–strain curves in figure 5, the effective Young's modulus E' decreases by four orders of magnitude when the composite is electrically activated. The measured moduli $E'_{\text{off}} = 0.86 \pm 0.10$ GPa and $E'_{\text{on}} = 95.2 \pm 10.5$ kPa are in reasonable agreement with the theoretical predictions $E'_{\text{off}} = 0.959$ GPa and $E'_{\text{on}} = 108.7$ kPa obtained from composite mechanics. Using the experimental methods described later, we measured that room temperature Field's metal and VHB tape have a Young's modulus of $E_{\text{F}} = 9.25 \pm 0.60$ GPa and $E_{\text{V}} = 128.4 \pm 24.3$ kPa, respectively. Therefore, the composite can be redesigned to have an even more dramatic change in effective modulus with an off/on ratio of approximately $E'_{\text{off}}/E'_{\text{on}} \sim \alpha_{\text{F}} E_{\text{F}}/(1-\alpha_{\text{F}})E_v$, where α_{F} is the cross-sectional area fraction of Field's metal. In the current design $\alpha_{\text{F}} = 0.104$ and so $E'_{\text{off}}/E'_{\text{on}} \sim 0.8 \times 10^4$. However, for a 60% area fraction, i.e. $\alpha_{\text{F}} = 0.6$, $E'_{\text{off}}/E'_{\text{on}} \sim 1.1 \times 10^5$. The same theoretical estimate may also be applied to stiffness tunable composites containing SMP.

In addition to accurately predicting tensile modulus, the theory also provides a reasonable estimate for the time $t = U/P$ required to activate the composite. The constant U represents the energy required to heat the composite to the melting point T_{m} or glass transition temperature T_{g} of the thermally responsive material. In the case of Field's metal and other low-melting-point alloys, U must include the latent heat absorbed during phase transition. The theoretical prediction is based on the assumption that temperature is uniform throughout the composite. This is reasonable since the heat is generated and diffused across the layers in the composite and the thicknesses of the layers are much smaller than the

planar dimensions. However, temperature is rarely uniform during Joule heating and a more general theory is needed to accurately predict the time t required to completely melt the alloy. Nonetheless, the simplified theory provides a reasonable estimate for t and suggests that the time t required to activate the composite prototype can be reduced by increasing the input current i, increasing the heater resistance R, and/or reducing the latent heat consumed by the phase transition. The latter can be accomplished by reducing the volume fraction β_F of Field's metal or replacing it with shape memory polymer. While reducing β_F will shorten the activation time, it will lead to a reduction in α_F and thus a decrease in the relative change in modulus E'_{off}/E'_{on}. It should be noted that $\rho_F c_F \sim \rho_V c_V$ and so changing the relative volume of Field's metal and VHB tape will not have a significant influence on the energy required to raise the temperature prior to the phase transition.

The resistance R of the heater is controlled by the length and cross-sectional area of the Galinstan channel. The coiled channel has a depth $h_G = 0.5$ mm, width $w_G = 1.27$ mm, turn spacing $s = 1.23$ mm, length $L_G = 218.7$ mm, and covers an area of approximately 400 mm^2. According to Ohm's law, $R = rL/w_G h_G = 0.10\ \Omega$, where $r = 2.9 \times 10^{-7}\ \Omega$ m is the resistivity of Galinstan. In contrast, for a 10 μm deep and 100 μm wide coiled channel with 100 μm spacing, the same area can be covered with a channel that has a total length of 2 m. This corresponds to a total resistance of 0.58 kΩ and implies that the composite can be activated with significantly less electrical current and in a shorter amount of time. Such an improvement is possible with the current masked deposition technique but requires the VHB elastomer to be patterned with surface engraving rather than complete cuts through the film thickness. Alternatively, the Galinstan may be replaced with a less conductive fluid or conductive elastomer. Also, in the case of Field's metal, the heater may be removed and the insulated Field's metal may be heated directly with electrical current.

Equations (1) and (2) are derived for tensile specimens with planar heating coils. The theory must be modified in order to predict elastic rigidity and activation time for other loading conditions and heater designs. For composites loaded in bending [10], E' must be replaced with an effective flexural rigidity D' that depends not only on the Young's modulus of the individual elements in the composite but also the area moment of inertia about the neutral bending axis. More accurate predictions can be obtained through computational modeling, although this will not directly lead to predictive algebraic formulas or scaling laws. The theory can also be improved by relaxing the assumption of uniform internal temperature. This will allow the theory to capture the inflection observed in figure 6 and better predict the time t required to achieve complete melting. In addition, the temperature distribution across the layers during phase change can also be analyzed. These calculations are important for reliably designing rigidity tunable materials and structures using VHB and phase-changing alloys, given the fact that VHB is functional only within a relatively narrow temperature range (from -35 to 110 °C). Because of the broad range of possible materials, designs, and length scales, theoretical models are of the greatest use if they can provide closed-form algebraic predictions and scaling laws without the need for experimental fitting or computationally intensive finite element modeling.

5. Rigidity tuning with shape memory polymer

Rigidity tuning with SMP has previously been demonstrated for thermally activated composites [9–11]. Referring to figure 7(a), we can use the fabrication method presented in section 2.1 to produce an RTC containing a 1 mm thick layer of SMP (SpinTech Ventures, Xenia, OH) and a liquid-phase Galinstan heater. The heater is sealed in VHB tape, which is adhesive and readily bonds to the SMP layer under light pressure. When electrically powered, the Galinstan coil heats the SMP above its glass transition temperature $T_g = 62$ °C. In this activated state, the composite becomes elastically compliant (figure 7(b)).

At room temperature, the SMP composite has a relatively high flexural rigidity and can support external load (figure 7(c)). As with other SMP-based RTC designs [9–11], the flexural rigidity diminishes significantly when the SMP is heated above its glass transition temperature (figure 7(d)). Moreover, since the SMP has the shape memory effect, the softened RTC can be deformed to a temporary shape upon cooling and revert to its original geometry upon heating again. In contrast, when Field's metal cools to room temperature, the solid-phase rigidity is restored but the composite does not return to its original shape. The shape memory effect makes SMP a promising candidate for 'artificial muscles' in bio-inspired robotics, human motor assistance, and other applications that require reversible shape and rigidity control.

6. Conclusion

In summary, we have demonstrated reversible elastic rigidity control with phase-changing alloy (Field's metal) and shape memory polymer using a soft-matter Joule heater. The heater and rigidity tunable material form a composite that becomes elastically soft and stretchable when activated with electrical current. With 6 A of current, the composite transforms from a rigid solid that resists stretching and bending into a soft elastomer that easily deforms. Because the heater does not contain any rigid or inextensible parts, it can accommodate the extreme elastic deformation of the stiffness tunable layer without breaking. Electronic functionality allows the composite to operate with battery power and on-board electronics and eliminates the need for pneumatic, fluidic, or motorized external hardware.

We also introduce a versatile method for rapidly producing elastomer composites embedded with low-melting-point metal. The composites may be scaled and patterned to any size or shape and can function in applications ranging from an artificial muscle for biologically inspired robots to a wearable brace for human motor assistance and injury prevention. Moreover, the composites contain no rigid or inextensible elements when fully activated. This soft-matter functionality is especially important for mechanical compatibility in assistive wearable technologies and emerging

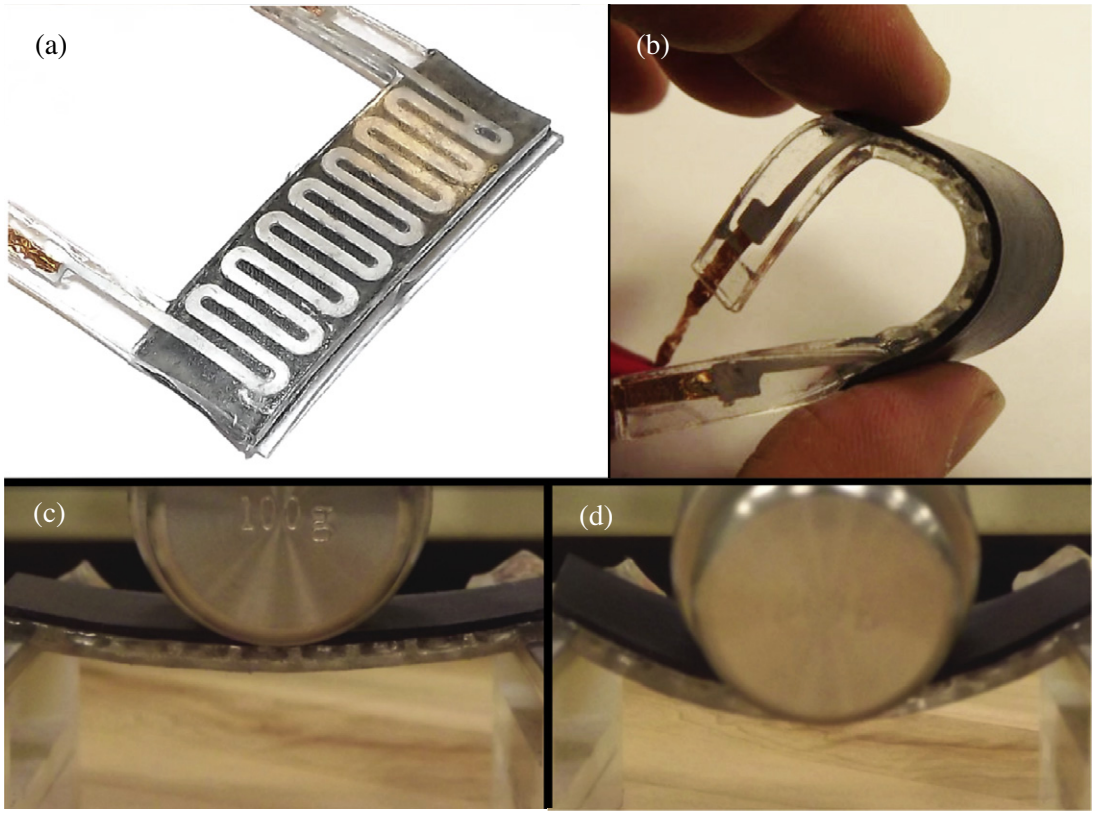

Figure 7. (a), (b) Rigidity tunable composite with embedded Galinstan heater and SMP. (c) At room temperature, the SMP is rigid and the composite can support flexural load. (d) When electrical current is supplied to the heater, the SMP softens and the composite bends.

soft robotics applications in which the host is naturally soft and elastic. Lastly, these composites are inexpensive and can be produced in minutes with masked deposition of liquid-phase metal alloy in laser-patterned films of acrylic elastomer (VHB^{TM} tape; 3M). Because the elastomer film bonds to itself through pressure-sensitive adhesion, each layer can be rapidly patterned, filled, wired, and sealed. This inexpensive and scalable fabrication method can be extended to other applications in soft-matter electronics and engineering, including liquid-phase gallium–indium circuits, sensor arrays, and radio-frequency identification.

The experimental results are in reasonable agreement with theoretical predictions derived from elementary composite mechanics and heat transfer. The theory may be generalized to obtain more accurate predictions and to examine a broad range of loading conditions and designs. In addition to improved theoretical models, future efforts will focus on implementation of actively tunable elastic rigidity for assistive wearable technologies and biologically inspired soft robots. We also plan to refine the masked deposition method to miniaturize the embedded features and incorporate a broader range of conductive and thermal or electrically responsive materials.

Acknowledgments

This work was supported by a Defense Advanced Research Projects Agency (DARPA) Young Faculty Award (Grant no. N66001-12-1-4255). The authors wish to thank Matthew Woodward (Carnegie Mellon University) for valuable insights on rigidity control with phase-changing alloy.

References

[1] Capadona J R, Shanmuganathan K, Tyler D J, Rowan S J and Weder C 2008 Stimuli-responsive polymer nanocomposites inspired by the sea cucumber dermis *Science* **319** 1370–4
[2] Shanmuganathan K, Capadona J R, Rowan S J and Weder C 2010 Biomimetic mechanically adaptive nanocomposites *Prog. Polym. Sci.* **35** 212–22
[3] Brown E, Rodenberg N, Amend J, Mozeika A, Steltz E, Zakin M R, Lipson H and Jaeger H M 2010 Universal robotic gripper based on the jamming of granular material *Proc. Natl Acad. Sci. USA* **107** 18809–14
[4] Trappe V, Prasad V, Cipelletti L, Segre P N and Weitz D A 2001 Jamming phase diagram for attractive particles *Nature* **411** 772–5
[5] Majidi C and Wood R J 2010 Tunable elastic stiffness with microconfined magnetorheological domains at low magnetic field *Appl. Phys. Lett.* **97** 164104
[6] Chen J Z and Liao W H 2010 Design, testing and control of a magnetorheological actuator for assistive knee braces *Smart Mater. Struct.* **19** 035029
[7] Varga Z, Filipcsei G and Zrinyi M 2006 Magnetic field sensitive functional elastomers with tuneable elastic modulus *Polymer* **47** 227–33
[8] Pratt G A and Williamson M M 1995 Series elastic actuators *Proc. IEEE/RSJ Conf. on Intelligent Robots and Systems; (Pittsburgh)*

[9] McKnight G, Doty R, Keefe A, Herrera G and Henry C 2010 Segmented reinforcement variable stiffness materials for reconfigurable surfaces *J. Intell. Mater. Syst. Struct.* **21** 1783–93

[10] Gandhi F and Kang S G 2007 Beams with controllable flexural stiffness *Active and Passiv Smart Structures and Integrated Systems; Proc. SPIE* **6525** 65251

[11] Clark W W, Brigham J C, Mo C and Joshi S 2010 Modeling of a high-deformation shape memory polymer locking link *Industrial and Commercial Applications of Smart Structures and Technologies; Proc. SPIE* **7645** 764507

[12] Henke M, Sorber J and Gerlach G 2012 Multi-layer beam with variable stiffness based on electroactive polymers *Electroactive Polymer Actuators and Devices; Proc. SPIE* **8340** 83401P

[13] Dickey M D, Chiechi R C, Larsen R J, Weiss E A, Weitz D A and Whitesides G M 2008 Eutectic gallium–indium (EGaIn): a liquid metal alloy for the formation of stable structures in microchannels at room temperature *Adv. Funct. Mater.* **18** 1097–104

[14] Cheng S and Wu Z 2012 Microfluidic electronics *Lab Chip* **12** 2782–91

[15] Siegel A C, Bruzewicz D A, Weibel D B and Whitesides G M 2007 Microsolidics: fabrication of three-dimensional metallic microstructures in poly(dimethylsiloxane) *Adv. Mater.* **19** 727–33

[16] Jeong S H, Hagman A, Hjort K, Jobs M, Sundqvist J and Wu Z 2012 Liquid alloy printing of microfluidic stretchable electronics *Lab Chip* **12** 4657–64

[17] Roberts P, Damian D D, Shan W L, Lu T and Majidi C 2013 Soft-matter capacitive sensor for measuring pressure and shear deformation *Proc. IEEE Int. Conf. on Robotics and Automation (ICRA) (Germany, 2013)* pp 3514–9